

Open Research Online

The Open University's repository of research publications and other research outputs

Cumulate causes for the low contents of sulfide-loving elements in the continental crust

Journal Item

How to cite:

Jenner, Frances Elaine (2017). Cumulate causes for the low contents of sulfide-loving elements in the continental crust. *Nature Geoscience*, 10(7) pp. 524–529.

For guidance on citations see [FAQs](#).

© [not recorded]



<https://creativecommons.org/licenses/by-nc-nd/4.0/>

Version: Accepted Manuscript

Link(s) to article on publisher's website:
<http://dx.doi.org/doi:10.1038/ngeo2965>

Copyright and Moral Rights for the articles on this site are retained by the individual authors and/or other copyright owners. For more information on Open Research Online's data [policy](#) on reuse of materials please consult the policies page.

oro.open.ac.uk

1 **Cumulate Causes for the Low Contents of Sulfide-loving**
2 **Elements in the Continental Crust**

3
4 Frances Elaine Jenner^{1,2}

5
6 ¹*School of Environment, Earth and Ecosystem Sciences, The Open University, Walton Hall,*
7 *Milton Keynes, Buckinghamshire, MK7 6AA.*

8
9 ²*Carnegie Institution for Science, Department of Terrestrial Magnetism, Washington DC*
10 *20015-1305, U.S.A.*

11
12 *Corresponding author: frances.jenner@open.ac.uk

13 *Phone: +44(0)1908 654334.*

14
15 **Keywords:** Oceanic crust; chalcophile; siderophile; continental crust; subduction;
16 sulfide

17
18 Summary: 233 words

19 Main text: 3384 words

20 Figures: 4

21 Supplementary Tables: 1

22

23 Despite their economic importance, surprisingly little is known about the
24 magmatic processes that cause the continental crust to become enriched in some
25 chalcophile (sulfide-loving) and siderophile (metal-loving) elements (CSE) and
26 depleted in others compared to the oceanic crust. This is in part due to limited
27 understanding of the partitioning of the CSE by both sulfide and non-sulfide
28 minerals. Using published datasets for global mid-ocean ridge basalts (MORB)
29 and subduction-related volcanic rocks, I show that mantle-derived melts
30 contributing to oceanic and continental crust formation rarely avoid sulfide-
31 saturation during cooling in the crust and, on average, subduction-zone magmas
32 fractionate sulfide at the base of the continental crust prior to ascent.
33 Differentiation of mantle-derived melts enriches lower crustal sulfide- and
34 silicate-bearing cumulates in some CSE compared to the upper crust. This
35 ‘storage’ predisposes the cumulate-hosted compatible CSE (e.g., Cu and Au) to
36 be recycled back into the mantle during subduction and delamination, resulting
37 in their low contents in the bulk continental crust and potentially contributing to
38 the scarcity of ore deposits in the upper continental crust. By contrast,
39 differentiation causes the upper oceanic and continental crust to become
40 enriched in ‘incompatible’ CSE (e.g., W) compared to the lower oceanic and
41 continental crust. Consequently, incompatible CSE are predisposed to become
42 enriched in subduction-zone magmas that contribute to continental crust
43 formation and are less susceptible to removal from the continental crust via
44 delamination compared to the compatible CSE.

45 Chalcophile and siderophile element (CSE) systematics of magmatic rocks can be
46 used to place constraints on a range of processes and parameters including the
47 evolution of the Earth’s mantle and crust, delamination, subduction, mantle redox and

48 the formation of ore deposits¹⁻¹⁰. Many of these constraints rely on knowledge of the
49 minerals partitioning the CSE and comparisons between the compositions of
50 subduction-zone magmas and MORB^{11, 12}. Ratios in average-MORB ('normal' (N)-
51 MORB) can be used to derive estimates of the composition of the MORB-source
52 depleted mantle⁹ and the primitive mantle¹, which are also important to comparative
53 geochemistry.

54 Because the contents of many CSE are hard to analyse accurately in rocks and
55 minerals¹³, compositions and ratios used for comparative geochemistry are often
56 based on scant datasets and/or relatively untested proxies^{4, 12, 14-16}. Consequently, there
57 remains a lack of consensus regarding which CSE are mobile during subduction and
58 whether the low [Cu] (where the brackets denote concentrations) of evolved
59 subduction-related magmas and the bulk continental crust can be attributed to sulfide
60 fractionation^{7, 8, 17}, accumulation and subsequent delamination² or alternatively, to
61 partitioning into exsolving fluids^{6, 18}. An added problem is that the CSE show a large
62 range in sulfide-silicate partition coefficients ($D^{sulf/sil}$) and many CSE partition into
63 non-sulfide minerals^{19, 20}, making CSE behaviour during magmatic processes difficult
64 to predict.

65 Using published datasets for natural and experimental materials^{7, 8, 19-31}, I show
66 that N-MORB values and certain ratios used for comparative geochemistry can be
67 misleading, because they do not sufficiently separate between mantle and crustal
68 processes. Both silicate and sulfide minerals host the CSE, so it is the bulk partition
69 coefficients (bulk-D) of the combined fractionating phases that determine the
70 concentration of the CSE in both the cumulates and fractionated liquids produced by
71 magmatic differentiation. The CSE hosted in the lower oceanic and continental crust
72 are recycled back into the mantle during subduction and delamination more efficiently

than the incompatible CSE that are enriched in the upper oceanic and continental crust. Hence, differentiation of both MORB and subduction-related magmas plays a role in determining the CSE composition of the mature continental crust.

OCEANIC CRUST

Average and log-normal mean distributions of elements in global MORB and various ratios are used to derive average-MORB and N-MORB estimates^{11, 12}. However, the [MgO] of average-MORB (7.6 wt.%¹¹) is lower than the bulk oceanic crust (≥ 10 wt.%)³². Lower oceanic crust cumulates (14.5 wt.% MgO³²) are the complementary products to the evolved basalts of the upper oceanic crust. Hence, average-MORB does not reflect the integrated composition of the bulk oceanic crust required for comparative geochemistry, which should correspond to the composition of parental-MORB prior to differentiation.

The composition of parental-MORB and the upper/lower oceanic crust distributions of the CSE are estimated as follows. Expanding on previous studies^{33, 34}, the least-squares fit line between the log-mean content of a given element (M) versus [MgO] in MORB glasses (see Fig. 1), together with the [MgO] of the bulk oceanic crust (10.0 wt.%) and average-MORB (7.6 wt.%) are used to derive the composition of average parental-MORB and evolved-MORB, respectively (Fig. 1, 2, Methods and Supplementary Table 1). The relationship between the slope of the best-fit line between individual CSE and [MgO] and the differences in compositions of evolved-MORB and parental-MORB are used to establish the relative bulk-D of the CSE during differentiation and the upper/lower oceanic crust distribution of CSE (Fig. 2a). For example, lithophile (silicate-loving) elements such as Co and Sc vary consistently with their bulk partition coefficients³³: Co (bulk-D=1.1) becomes slightly depleted (slope <0), while Sc (bulk-D=0.89) becomes slightly enriched (slope >0) in the melt

during MORB differentiation (Fig. 2a). Similarly, because the slope for chalcophile element Cu is positive (Fig. 1), the [Cu] of evolved-MORB (77 ppm) is significantly lower than parental-MORB (115 ppm). Copper is highly chalcophile²², therefore sulfide-bearing lower oceanic crust cumulates must have higher [Cu] than parental-MORB and the upper oceanic crust³⁵. Thus, the upper oceanic crust is enriched in incompatible CSE (slope <0), whereas the lower oceanic crust is enriched in compatible elements CSE (slope >0).

Evolved-MORB and N-MORB (log-normal mean MORB) is enriched in incompatible elements and depleted in compatible elements compared to parental-MORB (Fig. 2a). This degree of elemental fractionation (e.g., elevated La/Sm) cannot be achieved via simple fractional crystallization and is attributable to magma chamber recharge^{33, 34}. Hence, various proxies (e.g., Supplementary Table 1) used to derive representative CSE estimates for N-MORB¹², the depleted⁹ and primitive mantle¹ (e.g., Bi/Pb, Se/V, Rb/Tl), as redox proxies (e.g., V/Sc³), and/or as subduction tracers (e.g., Cs/Tl³¹, Bi/Nd⁶), should be replaced by ratios between elements with more comparable slopes (e.g., V/In instead of V/Sc). Consequently, parental-MORB is used as the normalising composition in the following discussion, as this composition provides a truer comparison between the fluxes from mantle-to-crust in different environments than N-MORB.

AFFINITIES OF THE CSE

The lithophile, chalcophile and siderophile affinities of many CSE during magmatic processes remain debated^{4, 14}. The slopes (relative bulk-D) can be compared with available $D^{sulf/sil}$ (Fig. 2) to place new constraints on the partitioning of the CSE during magmatic processes. For example, though Ge, Mn, Ga and Se have comparable bulk-Ds, $D^{sulf/sil}$ of Ge, Mn, Ga are significantly lower than Se (Fig.

2b), implying silicates, not sulfides, dominate the partitioning of Ge, Mn and Ga. Using the CSE with the highest $D^{sulf/sil}$ at a given slope ($Cu \approx Ag > Se > Bi > Pb > Tl$) as an approximation of the end-member ‘purely chalcophile’ trend, the partitioning of the majority of CSE during MORB differentiation and probably, mantle melting¹⁹, is either dominated or in part controlled by silicates and/or oxides. These elements are classified here as having ‘mixed-affinity’ (Fig. 2b).

The question remains as to whether sulfide is molten or crystalline in the mantle, which can be investigated by exploiting differences in the partitioning of CSE during the petrogenesis of MORB^{24, 36}. Sulfide-melt has similar $D^{sulf/sil}$ for Cu and Ag (Fig. 2), whereas crystalline-sulfide (e.g., chalcopyrite, Fig. 3) and silicates favour Cu over Ag^{24, 37}. The constant Cu/Ag of MORB with decreasing [MgO] (Fig. 3a) is attributable to sulfide-melt fractionation^{8, 22}. The presence of crystalline-sulfide²⁴, or the absence of sulfide in the mantle, should manifest as Cu/Ag variability in mantle-derived melts. However, the Cu/Ag of MORB varies by only 11%. Put into context, this is less variation than traditional canonical ratios Nb/U (16%) and Ce/Pb (17%) and approaches that of Zr/Hf (8%) and Nb/Ta (7%). The overlapping Cu/Ag of MORB, mantle xenoliths³⁸ and oceanic island basalts (Fig. 3) supports experimental studies predicting mantle sulfide is molten and is residual during melting³⁶.

SLAB VERSUS WEDGE COMPONENTS

The key difference between the petrogenesis of MORB and subduction-zone magmas is the introduction of extra components derived from the subducting slab. N-MORB-normalised plots and various ratios are commonly used to distinguish between slab (e.g., large ion lithophile elements, LILE) versus mantle wedge (e.g., high field strength elements, HFSE) contributions to subduction-zone magmas^{30, 39}. Corresponding enrichments and depletions in the parental-MORB-normalized

patterns of subduction-zone magmas and the bulk continental crust (Fig. 4), testify to the importance of subduction-related magmatism in contributing to continental crust formation²⁶.

Island arc magmas are often highly evolved and crystalline^{6, 30, 39}. Consequently, their compositions are skewed to higher incompatible/compatible element ratios compared to their parental melts and their bulk compositions often represent complex mixtures between the compositions of minerals and melt. In addition, datasets for island arc suites are often incomplete, missing critical CSE from the range plotted on Fig. 2 and/or are not of sufficient analytical quality¹³. By contrast, comprehensive datasets for primitive volcanic glasses from the Lau and Manus backarc basin (BAB) contain up to 8 and 9 wt.% MgO, respectively. They also have [H₂O] and trace element patterns akin to evolved Mariana-Izu island arc magmas (Fig. 4), demonstrating the influence of the underlying slab^{7, 8, 25}. Hence, a combination of BAB and island arc magmas are used here to constrain CSE behaviour during subduction-related magmatism.

Primitive BAB basalts normalised to parental-MORB are enriched in W, Mo, Tl, As, Pb Sb and Bi relative to the HFSE (Fig. 4), supporting previous conclusions that these CSE are mobile during subduction^{6, 15, 16, 28, 30}. By contrast, Sn-In-Zn-Cd-Ga-Mn-Ge-Co-Cu-Ag and Au⁷ show a relationship to neighbouring REE and HFSE that is comparable to parental-MORB (Fig. 4), implying that these CSE are relatively immobile during subduction and are largely derived from the mantle wedge component. Evolved (4.2-5.6 wt.% MgO) Mariana-Izu arc magmas show similar trace element patterns to primitive BAB (Fig. 4), but the absolute abundances of both the mobile and immobile elements are more comparable to evolved BAB, which is attributable to differentiation. For example, like primitive BAB (Fig. 3b), primitive

arc magmas (including those from the Mariana-Izu arc) have comparable or lower [Cu] than parental-MORB prior to differentiation (Supplementary Figure 1). Hence, the high Cu/Co of the Mariana-Izu samples (Fig. 4) can be attributed to enrichment during differentiation rather than Cu mobility during subduction.

Normalising primitive Lau BAB basalt to evolved-MORB (N-MORB) rather than parental-MORB results in a significant offset (Fig. 4). Because the evolved-MORB/parental-MORB offset increases in magnitude from Sc to Rb (Fig. 4), using N-MORB for normalisation results in an underestimation of (i) the fertility of the mantle wedge compared to the MORB-source mantle (e.g., using La/Sm, Nb/Zr or Nb/Yb³⁹), (ii) the slab-to-mantle wedge flux of incompatible elements (e.g., using Pb/Yb, Th/Yb, and Cs/Tl^{4, 6, 39}) and (iii) the magnitude of the incompatible element enrichments in the bulk continental crust compared to the bulk oceanic crust. The opposite problem pertains to elements enriched in the lower oceanic crust, which, in addition to the evolved nature of many arc magmas, has contributed to disagreements regarding, for example, whether Cu is mobile^{6, 16} or not^{2, 7, 8} during subduction.

CONTROLS ON THE SLAB-TO-MANTLE WEDGE FLUX

The order of enrichment of As>Tl>Pb>Sb>Bi in primitive Manus BAB/parental-MORB (Fig. 5a) is similar to the order of enrichment in evolved-MORB/parental-MORB (Fig. 2). Hence, the upper oceanic crust appears to source the flux of incompatible CSE to the mantle wedge. This implies that the majority of As-Tl-Pb-Sb-Bi host-phases in the upper oceanic crust are unstable during subduction, permitting their mobilization by slab-derived fluids. Obvious candidates are low-temperature hydrothermal sulphides, sulfosalts and serpentinite minerals^{40, 41}. This conclusion is supported Pb isotope systematics of Mariana arc magmas, which links the source of the unradiogenic Pb in the fluid-component to the subducting MORB-

component²⁸. However, an overprinting sediment melt component is also required to explain the range of Pb and Tl isotope compositions of Mariana and other arc magmas^{4, 28} and probably, variations in [As]-[Tl]-[Pb]-[Sb]-[Bi] of global subduction-zone magmas.

Tungsten and Mo have lower bulk-Ds during MORB differentiation than Pb and Sb, respectively, (Fig 2), but are less mobile during subduction (Fig. 5). Hence, minerals more stable than hydrothermal sulfides (e.g., rutile²⁸) probably host a proportion of the W and Mo during subduction.

Primitive BAB have [Cu]-[Ag]-[Se] (also [Re]-[Pt]-[Au]⁸) comparable to parental-MORB (Fig. 4-5), implying limited mobility during subduction. Similarly, global arc datasets (e.g., Supplementary Figure 1) have been used to argue that Cu is immobile during subduction^{2, 17}. Hence, ‘trapping’ of Cu-Se-Ag-Au in magmatic sulphides in the lower oceanic crust prior to subduction might predispose the cumulate-hosted CSE to be recycled back into the mantle during subduction more efficiently than the CSE that are hosted in the upper oceanic crust (Fig. 2b). The MORB-like Cu/Ag of primitive BAB (Fig. 3) suggests residual sulfide-melt in the mantle wedge dominates Au>Ag≈Cu>Se partitioning. Thus, the subtly higher Cu/Se and Ag/Se (Fig. 5a) and the lower Nb/Zr of primitive-BAB compared to parental-MORB is consistent with either higher degrees of partial melting or the more depleted nature of their mantle wedge compared to the MORB-source mantle⁸.

Bismuth is compatible in magmatic sulfides and has a comparable bulk-D to Se during MORB differentiation (Fig. 2), but unlike Cu-Se-Ag-Au, it is mobile during subduction (Fig. 4-5). Despite sulfide-fractionation, volcanic glass (comprising up to 20 vol% of the extrusive oceanic crust⁴²) hosts a significant proportion of the Bi>Se>Cu~Ag of the bulk oceanic crust prior to hydrothermal alteration and

precipitation of numerous types of hydrothermal sulfides. CSE-hosting minerals found in sulfide ore deposits⁴³ have an extremely large range in melting temperatures. Hence, the diverging behaviour of Se and Bi during subduction suggests that Se-Cu-Ag-Au-hosting hydrothermal sulfides (e.g., chalcopyrite) are more stable than the predominantly low-temperature Bi-Pb-Tl-Sb-As-hosting hydrothermal sulfides and sulfosalts in the upper oceanic crust during subduction.

Despite their higher fO_2 than MORB and consequently, higher S solubility⁴⁴, BAB magmas discussed here have MORB-like [S] (prior to degassing on eruption), implying limited S release to the wedge during BAB magmatism⁸. However, analyses of mineral-hosted melt inclusions show that some (but not all) arc magmas are enriched in S compared to MORB⁴⁵. Hence, S mobility during subduction appears variable.

Most of the ‘mixed-affinity’ CSE (Fig. 2b) appear relatively immobile during subduction (Fig. 4). Analyses of [Co], [Zn], [Ga], [Ge] in accessory minerals in eclogites suggest that non-sulfide minerals such as clinopyroxene, garnet, phengite, apatite, rutile and allanite host the mixed-affinity CSE during subduction⁴⁶ (and by inference Sn, In and Cd). Considering a broad range of silicate-hosted (Zn, Sn, In, Cd, Ga, Ge, Co) and sulfide-hosted (Cu, Ag, Se, Au) CSE have comparable patterns in primitive subduction-zone magmas and parental-MORB, both the mantle wedge and the MORB-source mantle probably contain residual pyroxene and sulfide.

In summary, both oceanic crust differentiation (i.e., the upper/lower crust distributions of CSE) and the mineral affinities of the CSE during differentiation and alteration of the oceanic crust (Fig. 2b) predispose the CSE to be either mobile or immobile during subduction.

CONTINENTAL CRUST

The continental crust has a bulk andesitic composition approximating evolved rather than primitive subduction-related magmas²⁶ (Fig. 4). This offset is often attributed to delamination of cumulates from the base of the continental crust²⁶. Delamination of sulfide-bearing cumulates has also been proposed to account for the Cu-deficit of the continental crust and the first Pb paradox (location of the missing unradiogenic Pb)^{2, 47}. However, the role of sulfide fractionation during arc magma differentiation remains debated. For example, the low [CSE] of evolved subduction-zone magmas is often attributed to partitioning into exsolving volatile phase(s) rather than sulfide fractionation^{6, 18}. Hence, understanding the behaviour of the CSE during differentiation of subduction-related magmas might provide clues towards understanding the composition of the mature continental crust.

Tholeiitic BAB magmas and arc magma suites developed on crust that is <20 km thick (e.g., Mariana, Supplementary Figure 1), show an initial increase (sulfide under-saturated) then concomitant decrease in [FeO] and [Cu] at ~4-5 wt.% MgO (Fig. 3b), which has been attributed to magnetite-driven reduction of the melt triggering sulfide-saturation during differentiation of high fO_2 melts^{7, 8, 17}. For example, the sample from the Manus BAB with the highest [Cu] (green circle, Fig. 3b), also has higher [Se] (and hence S prior to degassing on eruption; see modelling in Refs^{7, 8, 25}), [Ag] and [Au] than the most primitive BAB from the region (Fig. 3c). Together with the constant Cu/Se (Jenner et al.,⁸ their Figure 8), these systematics indicate that the evolving melts were initially sulfide-under-saturated. As the magma evolves, magnetite-triggered sulfide-fractionation causes a significant drop in [Se] (and by proxy [S])^{7, 8, 25}, [Ag], [Au], [Cu] (Fig. 3c). Unlike MORB, BAB suites show a drop in Cu/Ag following sulfide-fractionation (Fig. 3a), implying fractionation of crystalline-sulfide as opposed to sulfide-melt^{7, 8}.

Alternatively, Sun et al.¹⁸ used [S] versus [SiO₂] systematics to argue that the Manus BAB melts contained insufficient S to achieve sulfide-saturation during differentiation and consequently, attributed the drop in [CSE] to partitioning into exsolving fluids. This interpretation is contrary to modelling, based on experimental constraints (Figure 8b of Ref.⁷), which shows that the drop in [CSE] during differentiation of the Manus suite coincides with the melts achieving the [Cu]+[S] necessary for sulfide-saturation (see^{7,8,17} for detailed discussion). Furthermore, S-Se-Fe-Cu-Ag-Au systematics of the Manus suite, together with the differences in [S] between mineral-hosted melt inclusions and volcanic glasses indicate S degassing took place after sulfide fractionation^{7,8,17}.

Arc magmas erupted through >30 km of crust that show calc-alkaline differentiation trends (e.g., the Andes) fractionate sulfide at higher [MgO] (≥8 wt.%) than arc tholeiitic suites erupted through <20 km of crust¹⁷ (Supplementary Figure 1b). This difference has been attributed to the higher [H₂O] and *f*O₂ of melts evolving in thicker arcs and consequently, earlier magnetite fractionation¹⁷. Recent experimental data demonstrating the sulfide stability field shifts towards more oxidising conditions with increasing pressure⁴⁴ may offer an alternative explanation: high-pressure differentiation causes magmas erupting through >30 km of crust to saturate in sulfide regardless of their H₂O, *f*O₂ or consequently, the timing of magnetite fractionation.

The bulk and lower continental crust has a CSE pattern and Cu/Ag strikingly similar to the most evolved (<1 wt.% MgO) sulfide-saturated BAB rhyolites (Figs. 3 and 5). Consequently, crystalline-sulfide fractionation appears to dominate during continental crust formation, whereas sulfide-melt fractionation dominates during oceanic crust formation. The low Cu/Ag of the lower continental crust indicates

average arc magmas differentiate at the base of the crust long enough to permit significant crystalline-sulfide fractionation prior to ascent to higher crustal levels: a conclusion that is complementary to ‘deep crustal hot-zone’ models⁴⁸ and potentially accounts for the lower [Cu] of even ‘primitive’ arc magmas compared to parental-MORB (Supplementary Figure 1). The lower and bulk continental crust has significantly higher [MgO] than BAB rhyolites, despite their comparable Cu/Ag (Fig. 3a). This difference suggests that continental crust formation is dominated by addition of arc magmas with differentiation histories akin to calc-alkaline series magmas erupting through >30 km of crust (i.e., sulfide-saturated at ≥ 8 wt.% MgO rather than ~ 4 wt.% MgO). Considering H₂O solubility increases with increasing pressure⁴⁹, it is unlikely that partitioning of CSE into exsolving fluids (e.g.,¹⁸) in the lowermost crust (rather than magmatic sulfides) can account for the differences in CSE systematics between magmas erupting through <20 km versus >30 km of crust.

Crystalline sulfide accumulation should cause subduction-related cumulates to have higher Cu/Ag than MORB and primitive BAB. Consequently, the low Cu/Ag of the bulk and lower continental crust provides strong support for delamination models. Using constraints provided here, mass balance deficits attributable to delamination probably exist for most CSE, which is consistent with the comparable [CSE] of the bulk continental crust compared to evolved rather than primitive BAB magmas (Fig. 3c). Given that all CSE are less enriched in rhyolites compared to U and Th (Fig. 3c), a proportion of even the incompatible CSE (e.g., Pb) is likely hosted in the lower continental crust prior to delamination (e.g., Th/Pb and U/Pb show a significant increase from 0.135 and 0.085 in the most primitive sample to 0.260 and 0.174 in the most evolved sample, respectively). This finding supports claims that delamination may contribute to the first Pb paradox^{2, 47}.

ORE DEPOSITS

It is perhaps unsurprising that porphyry ore-deposits in the upper continental crust are rare considering: (i) Cu-Ag-Au are immobile during subduction; (ii) mantle-melts rarely avoid sulfide-saturation during differentiation; (iii) Cu-Au-Ag are hosted by minerals in the lower continental crust, which can be delaminated. Given the effects of pressure on the sulfide stability field⁴⁴, magmas intruded into the lower continental crust are unlikely to destabilise/assimilate pre-existing sulfides. However, because the sulfide stability field shifts to lower fO_2 with decreasing pressure, rapid ascent of magmas could permit subduction-zone magmas to safely reach the upper continental crust without sustaining significant sulfide fractionation and/or would cause dissolution of entrained sulfides. In the upper continental crust numerous processes can be invoked to either decrease the chances of sulfide-saturation during differentiation (e.g., S degassing^{8, 44}) or reverse the effects of sulfide-saturation (e.g., sulfide dissolution by subsequent exsolving volatiles⁵), which may account for why porphyries are typically located at crustal depths of <10 km⁵. Such processes would generate co-enrichment in elements that are highly incompatible (e.g., Mo, W) and highly chalcophile (e.g., Cu, Au), which are characteristics of porphyries that are distinct from the typical upper/lower crust distribution of CSE (Fig. 3).

Mixed-affinity CSE, such as In and Zn, are not typically enriched in porphyries, implying their partitioning into silicates and/or oxides rather than less stable sulfides limits their potential to partition into late-stage exsolving fluids. However, these mixed-affinity CSE are likely released during crustal anatexis, which, in addition to differences in the fractionating mineral assemblages between mantle versus predominantly crustal melts, might explain why In-Zn-Sn mineralisation is associated with granitic intrusions⁵⁰, rather than subduction-related porphyries.

References

1. Palme, H. & O'Neill, H. St C. in Treatise on Geochemistry: The Mantle and Core (ed. Carlson, R.W.) 1-39 (Elsevier-Pergamon, Oxford, 2014).
2. Lee, C.-T.A. et al. Copper Systematics in Arc Magmas and Implications for Crust-Mantle Differentiation. *Science* **336**, 64-68 (2012).
3. Lee, C.-T.A., Leeman, W.P., Canil, D. & Li, Z.-X.A. Similar V/Sc Systematics in MORB and Arc Basalts: Implications for the Oxygen Fugacities of their Mantle Source Regions. *Journal of Petrology* **46**, 2313-2336 (2005).
4. Nielsen, S.G. et al. Tracking along-arc sediment inputs to the Aleutian arc using thallium isotopes. *Geochimica et Cosmochimica Acta* **181**, 217-237 (2016).
5. Wilkinson, J.J. Triggers for the formation of porphyry ore deposits in magmatic arcs. *Nature Geoscience* **6**, 917-925 (2013).
6. Timm, C., de Ronde, C.E.J., Leybourne, M.I., Layton-Matthews, D. & Graham, I.J. Sources of Chalcophile and Siderophile Elements in Kermadec Arc Lavas. *Economic Geology* **107**, 1527-1538 (2012).
7. Jenner, F.E., O'Neill, H. St C., Arculus, R.J. & Mavrogenes, J.A. The Magnetite Crisis in the Evolution of Arc-related Magmas and the Initial Concentration of Au, Ag, and Cu. *Journal of Petrology* **51**, 2445-2464 (2010).
8. Jenner, F.E. et al. The competing effects of sulfide saturation versus degassing on the behavior of the chalcophile elements during the differentiation of hydrous melts. *Geochemistry, Geophysics, Geosystems* **16**, 1490-1507 (2015).

- 372 9. Salters, V.J.M. & Stracke, A. Composition of the depleted mantle.
373 *Geochemistry geophysics geosystems* **5**, Q05004 (2004).
- 374 10. Richards, J.P. The oxidation state, and sulfur and Cu contents of arc
375 magmas: implications for metallogeny. *Lithos* **233**, 27-45 (2015).
- 376 11. Gale, A., Dalton, C.A., Langmuir, C.H., Su, Y. & Schilling, J.-G. The mean
377 composition of ocean ridge basalts. *Geochemistry, Geophysics, Geosystems*,
378 489-518 (2013).
- 379 12. Arevalo, R. & McDonough, W.F. Chemical variations and regional diversity
380 observed in MORB. *Chemical Geology* **271**, 70-85 (2010).
- 381 13. Jenner, F.E. & Arevalo, R.D. Major and Trace Element Analysis of Natural
382 and Experimental Igneous Systems using LA-ICP-MS. *Elements* **12**, 311-
383 316 (2016).
- 384 14. Yi, W. et al. Cadmium, indium, tin, tellurium, and sulfur in oceanic basalts:
385 Implications for chalcophile element fractionation in the Earth. *J. Geophys.*
386 *Res.* **105**, 18927-18948 (2000).
- 387 15. Jochum, K.P. & Hofmann, A.W. Constraints on earth evolution from
388 antimony in mantle-derived rocks. *Chemical Geology* **139**, 39-49 (1997).
- 389 16. Noll, J.P.D., Newsom, H.E., Leeman, W.P. & Ryan, J.G. The role of
390 hydrothermal fluids in the production of subduction zone magmas:
391 Evidence from siderophile and chalcophile trace elements and boron.
392 *Geochimica et Cosmochimica Acta* **60**, 587-611 (1996).
- 393 17. Chiaradia, M. Copper enrichment in arc magmas controlled by overriding
394 plate thickness. *Nature Geoscience* **7**, 43-46 (2014).
- 395 18. Sun, W. et al. Porphyry deposits and oxidized magmas. *Ore Geology*
396 *Reviews* **65**, Part 1, 97-131 (2015).

- 397 19. Witt-Eickschen, G., Palme, H., O'Neill, H. St C. & Allen, C.M. The
398 geochemistry of the volatile trace elements As, Cd, Ga, In and Sn in the
399 Earth's mantle: New evidence from in situ analyses of mantle xenoliths.
400 *Geochimica et Cosmochimica Acta* **73**, 1755-1778 (2009).
- 401 20. Tanner, D., Mavrogenes, J.A., Arculus, R.J. & Jenner, F.E. Trace Element
402 Stratigraphy of the Bellevue Core, Northern Bushveld: Multiple Magma
403 Injections Obscured by Diffusive Processes. *Journal of Petrology* **55**, 859-
404 882 (2014).
- 405 21. Jenner, F.E. & O'Neill, H. St C. Analysis of 60 Elements in 616 Ocean Floor
406 Basaltic Glasses. *Geochemistry geophysics geosystems* **13**, Q02005 (2012).
- 407 22. Patten, C., Barnes, S.-J., Mathez, E.A. & Jenner, F.E. Partition coefficients of
408 chalcophile elements between sulfide and silicate melts and the early
409 crystallization history of sulfide liquid: LA-ICP-MS analysis of MORB
410 sulfide droplets. *Chemical Geology* **358**, 170-188 (2013).
- 411 23. Kiseeva, E.S. & Wood, B.J. The effects of composition and temperature on
412 chalcophile and lithophile element partitioning into magmatic sulphides.
413 *Earth and Planetary Science Letters* **424**, 280-294 (2015).
- 414 24. Li, Y. & Audétat, A. Partitioning of V, Mn, Co, Ni, Cu, Zn, As, Mo, Ag, Sn, Sb,
415 W, Au, Pb, and Bi between sulfide phases and hydrous basanite melt at
416 upper mantle conditions. *Earth and Planetary Science Letters* **355-356**,
417 327-340 (2012).
- 418 25. Jenner, F.E. et al. Chalcophile element Systematics in Volcanic Glasses
419 from the Northwestern Lau Basin. *Geochemistry geophysics geosystems* **13**,
420 Q06014 (2012).

- 421 26. Rudnick, R.L. & Gao, S. in *Treatise on Geochemistry: The Crust* (ed.
422 Rudnick, R.L.) 1-64 (Elsevier, Oxford, 2003).
- 423 27. Dare, S.S., Barnes, S.-J. & Prichard, H. The distribution of platinum group
424 elements (PGE) and other chalcophile elements among sulfides from the
425 Creighton Ni–Cu–PGE sulfide deposit, Sudbury, Canada, and the origin of
426 palladium in pentlandite. *Mineralium Deposita* **45**, 765-793 (2010).
- 427 28. Freymuth, H., Vils, F., Willbold, M., Taylor, R.N. & Elliott, T. Molybdenum
428 mobility and isotopic fractionation during subduction at the Mariana arc.
429 *Earth and Planetary Science Letters* **432**, 176-186 (2015).
- 430 29. Freymuth, H., Ivko, B., Gill, J.B., Tamura, Y. & Elliott, T. Thorium isotope
431 evidence for melting of the mafic oceanic crust beneath the Izu arc.
432 *Geochimica et Cosmochimica Acta* **186**, 49-70 (2016).
- 433 30. Elliott, T., Plank, T., Zindler, A., White, W. & Bourdon, B. Element transport
434 from slab to volcanic front at the Mariana arc. *Journal of Geophysical*
435 *Research: Solid Earth* **102**, 14991-15019 (1997).
- 436 31. Prytulak, J., Nielsen, S.G., Plank, T., Barker, M. & Elliott, T. Assessing the
437 utility of thallium and thallium isotopes for tracing subduction zone
438 inputs to the Mariana arc. *Chemical Geology* **345**, 139-149 (2013).
- 439 32. White, W.M. & Klein, E.M. in *Treatise on Geochemistry (Second Edition):*
440 *The Crust* (ed. Turekian, H.D.H.K.) 457-496 (Elsevier, Oxford, 2014).
- 441 33. O'Neill, H. St C. & Jenner, F.E. The global pattern of trace-element
442 distributions in ocean floor basalts. *Nature* **491**, 698-704 (2012).
- 443 34. O'Neill, H. St C. & Jenner, F.E. Causes of the Compositional Variability
444 among Ocean Floor Basalts. *Journal of Petrology* **57**, 2163-2194 (2017).

- 445 35. Li, Y. Chalcophile element partitioning between sulfide phases and
446 hydrous mantle melt: Applications to mantle melting and the formation of
447 ore deposits. *Journal of Asian Earth Sciences* **94**, 77-93 (2014).
- 448 36. Zhang, Z. & Hirschmann, M.M. Experimental constraints on mantle sulfide
449 melting up to 8 GPa. *American Mineralogist* **101**, 181-192 (2016).
- 450 37. Adam, J. & Green, T. Trace element partitioning between mica- and
451 amphibole-bearing garnet lherzolite and hydrous basanitic melt: 1.
452 Experimental results and the investigation of controls on partitioning
453 behaviour. *Contributions to Mineralogy and Petrology* **152**, 1-17 (2006).
- 454 38. Wang, Z. & Becker, H. Abundances of Ag and Cu in mantle peridotites and
455 the implications for the behavior of chalcophile elements in the mantle.
456 *Geochimica et Cosmochimica Acta* **160**, 209-226 (2015).
- 457 39. Pearce, J.A., Stern, R.C., Bloomer, S.H. & Fryer, P. Geochemical mapping of
458 the Mariana arc-basin system: Implications for the nature and
459 distribution of subduction components. *Geochemistry geophysics*
460 *geosystems* **6**, Q07006 (2005).
- 461 40. Guillot, S. & Hattori, K. Serpentinites: Essential Roles in Geodynamics, Arc
462 Volcanism, Sustainable Development, and the Origin of Life. *Elements* **9**,
463 95-98 (2013).
- 464 41. Peucker-Ehrenbrink, B., Hofmann, A.W. & Hart, S.R. Hydrothermal lead
465 transfer from mantle to continental crust: the role of metalliferous
466 sediments. *Earth and Planetary Science Letters* **125**, 129-142 (1994).
- 467 42. Staudigel, H. in *Treatise on Geochemistry (Second Edition): The Crust*
468 (eds. Holland, H.D. & Turekian, K.K.) 583-606 (Elsevier, Oxford, 2014).

- 469 43. Tomkins, A.G., Pattison, D.R.M. & Frost, B.R. On the Initiation of
470 Metamorphic Sulfide Anatexis. *Journal of Petrology* **48**, 511-535 (2007).
- 471 44. Matjuschkin, V., Blundy, J.D. & Brooker, R.A. The effect of pressure on
472 sulphur speciation in mid- to deep-crustal arc magmas and implications
473 for the formation of porphyry copper deposits. *Contributions to*
474 *Mineralogy and Petrology* **171**, 1-25 (2016).
- 475 45. Wallace, P.J. Volatiles in subduction zone magmas: concentrations and
476 fluxes based on melt inclusion and volcanic gas data. *Journal of*
477 *Volcanology and Geothermal Research* **140**, 217-240 (2005).
- 478 46. Hermann, J. Allanite: thorium and light rare element carrier in subducted
479 crust. *Chemical Geology* **192**, 287-306 (2002).
- 480 47. Blichert-Toft, J. et al. Large-scale tectonic cycles in Europe revealed by
481 distinct Pb isotope provinces. *Geochemistry, Geophysics, Geosystems*, 3854-
482 3864 (2016).
- 483 48. Annen, C., Blundy, J.D. & Sparks, R.S.J. The Genesis of Intermediate and
484 Silicic Magmas in Deep Crustal Hot Zones. *Journal of Petrology* **47**, 505-
485 539 (2006).
- 486 49. Plank, T., Kelley, K.A., Zimmer, M.M., Hauri, E.H. & Wallace, P.J. Why do
487 mafic arc magmas contain ~4 wt% water on average? *Earth and Planetary*
488 *Science Letters* **364**, 168-179 (2013).
- 489 50. Simons, B., Andersen, J.C.Ø., Shail, R.K. & Jenner, F.E. Fractionation of Li,
490 Be, Ga, Nb, Ta, In, Sn, Sb, W and Bi in the peraluminous Early Permian
491 Variscan granites of the Cornubian Batholith: Precursor processes to
492 magmatic-hydrothermal mineralisation. *Lithos* **278-281**, 491-512
493 (2017).

Acknowledgements

Hugh O'Neill, Julie Prytulak, Roberta Rudnick, Helen Williams, Simon Kelley, Erik Hauri, Julie Bryce, Tim Elliott, Jon blundy, Nick Rogers, Nigel Harris, Rick Carlson and Chris Hawkesworth are thanked for motivational and/or derogatory comments that helped improve my ability to deliver an accessible manuscript. I would like to thank the NERC (grant reference NE/M000427/1 and NE/M010848/1) for funding. Bernie Wood, Yuan Li, Al Hoffmann, Francis Albarède, an anonymous reviewer and editor Amy Whitchurch are thanked for constructive reviews and comments on earlier versions of this manuscript.

Competing financial interests: The author declares no competing financial interests.

Supplementary Materials are linked to the online version of the paper at www.nature.com/nature.

FIGURE CAPTIONS

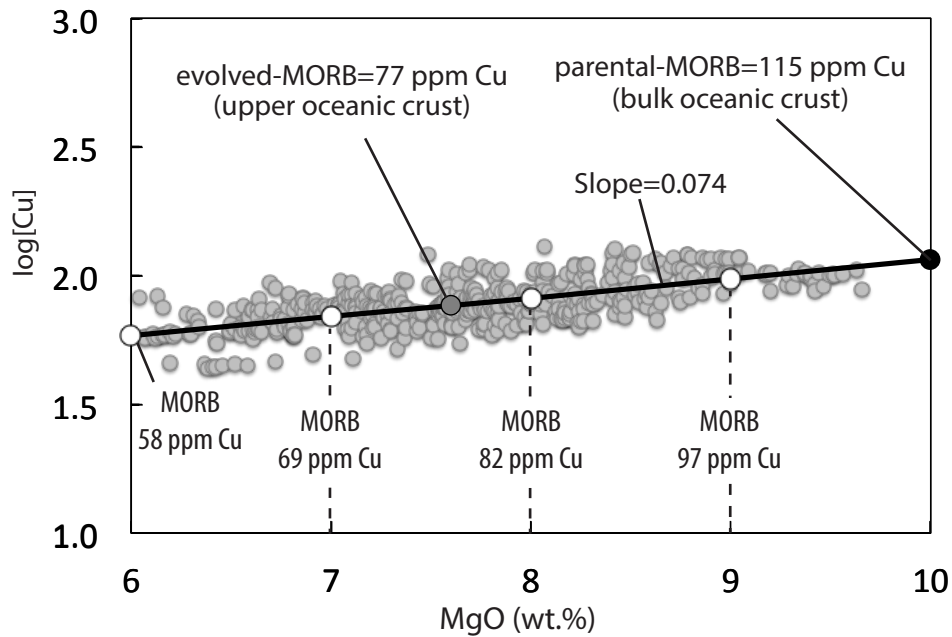


Figure 1: Global MORB log[Cu] versus [MgO]. The slope (0.074) of the best-fit line through the global MORB array (490 samples, data filtering methods described in Methods), together with the [Cu] at various [MgO] along the trend, is used to estimate the composition of parental-MORB (10 wt.% MgO: a proxy for the bulk oceanic crust composition) and evolved-MORB (7.6 wt.% MgO: a proxy for the composition of the upper oceanic crust). [Cu] versus [MgO] shows a positive correlation because Cu is a compatible element (bulk- $D \gg 1$).

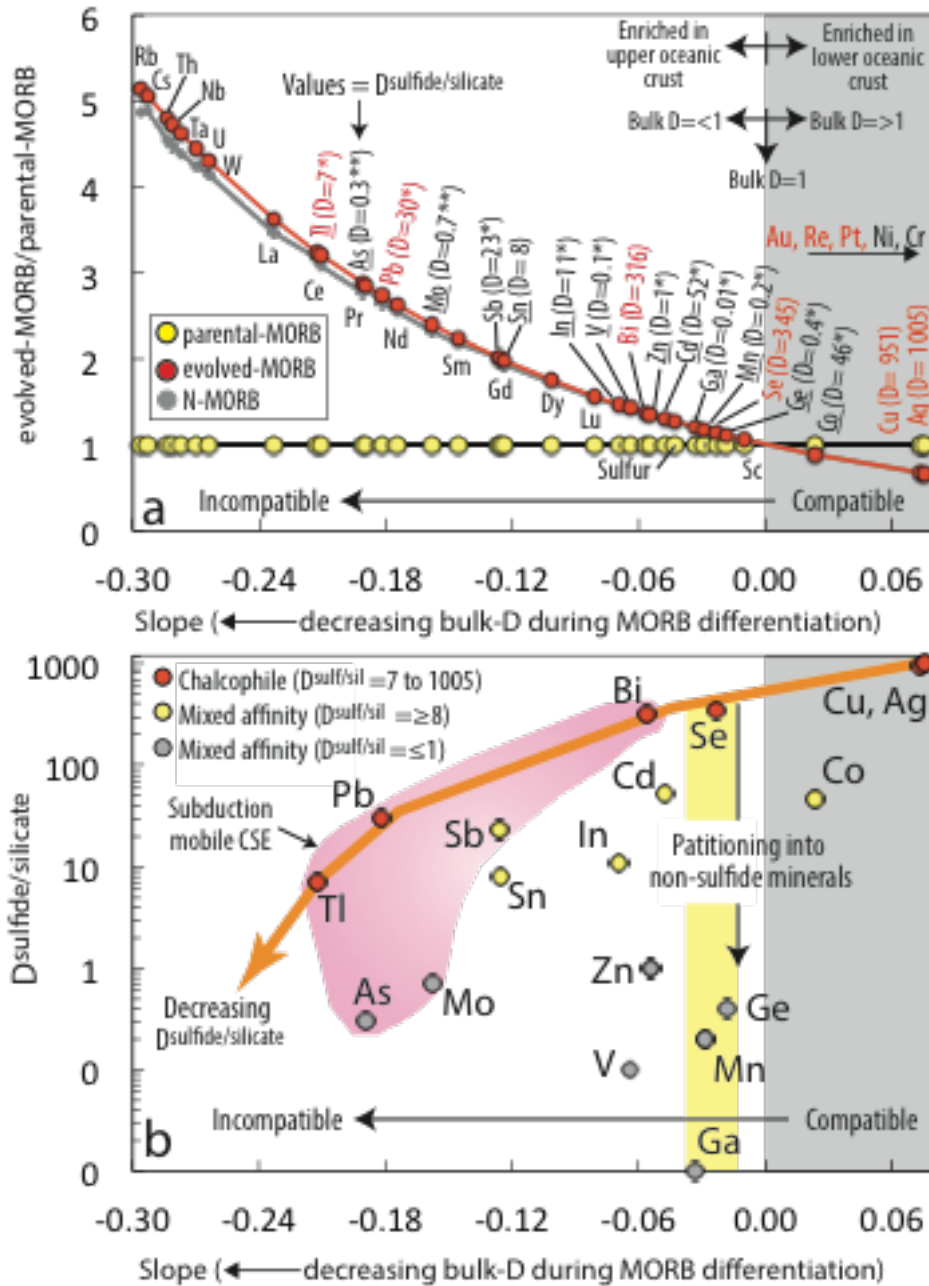


Figure 2: CSE partitioning during MORB differentiation; a) Elements with negative slopes are enriched whereas those with positive slopes are depleted during MORB differentiation. $D^{\text{sulph/sil}}$ for MORB-hosted sulphides²² except ‘*’ derived using the $D^{\text{sulph/sil}}$ calculator²³, (for a melt with 9 wt.% FeO_{TOT} and [Ni] and [Cu] from MORB-hosted sulphide RC28-02-07re-G1²²) and ‘**’ from experiment LY-29²⁴, which has $D^{\text{sulph/sil}}$ Cu/Ag comparable to MORB sulphides. b) scatter between

$D^{sulph/sil}$ versus slopes can be attributed to the mixed-affinities of CSE for sulfides and non-sulfide minerals, except potentially those with the highest $D^{sulph/sil}$ at a given slope (orange arrow).

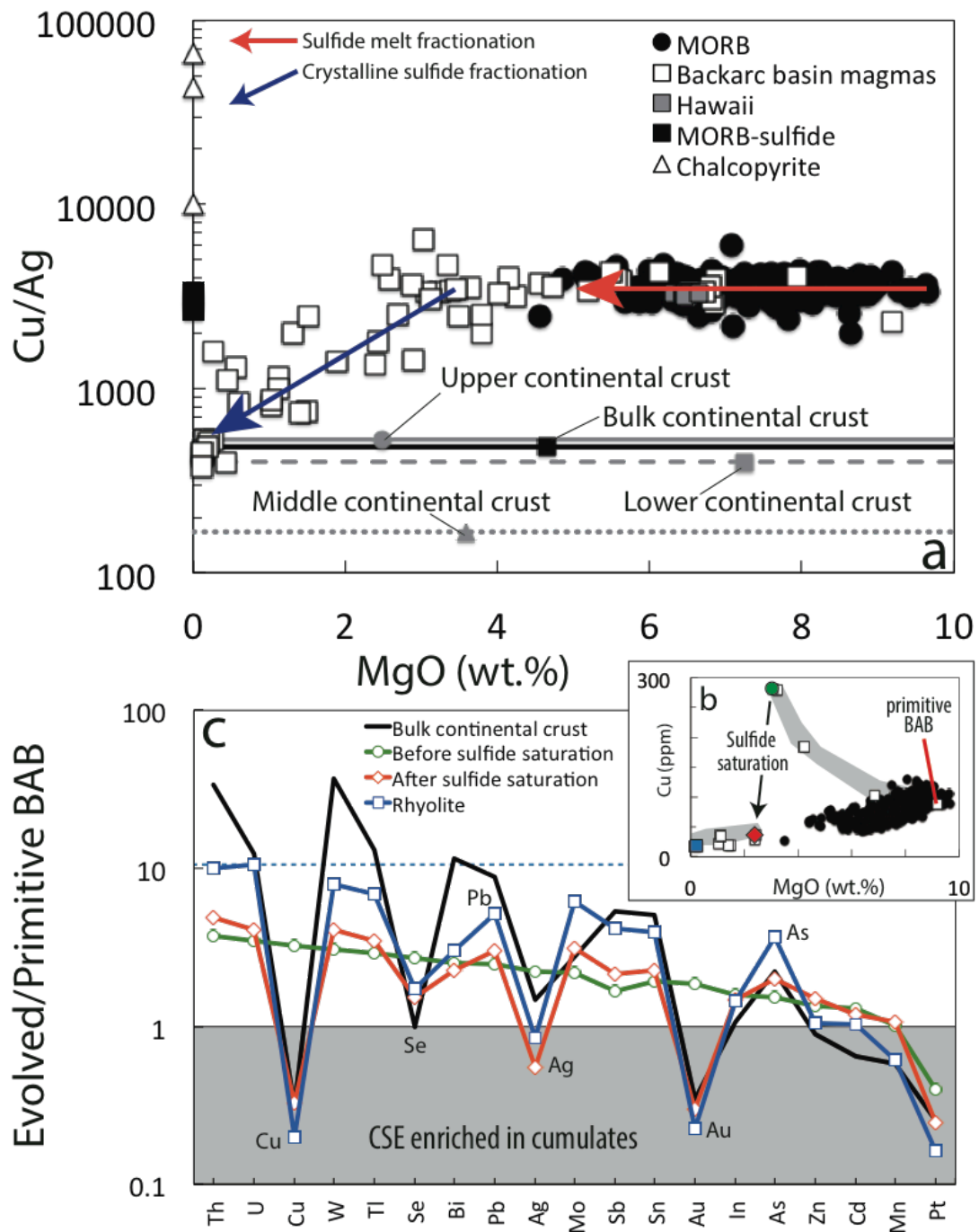


Figure 3: CSE partitioning during crustal differentiation. a) Cu/Ag versus [MgO] of MORB²¹, MORB-hosted sulfide²², Hawaiian basalts²⁵, BAB magmas^{7, 8}, continental crust estimates²⁶ and chalcopyrite²⁷ (see text for discussion). b) Unlike MORB, Manus BAB are initially sulphide under-saturated ([Cu] increases with decreasing [MgO]), until sulphide-saturation at <4 wt.% MgO. c) Samples from along the [Cu] versus [MgO] Manus trend (see b) and the bulk continental crust estimate are normalised to the most primitive Manus sample to constrain the partitioning of the CSE during differentiation of subduction-related melts (e.g., [Cu] is higher before sulfide-saturation and lower after sulfide-saturation). Note, [Pt] is depleted by partitioning into Pt-rich alloy^{7, 8} prior to sulfide saturation.

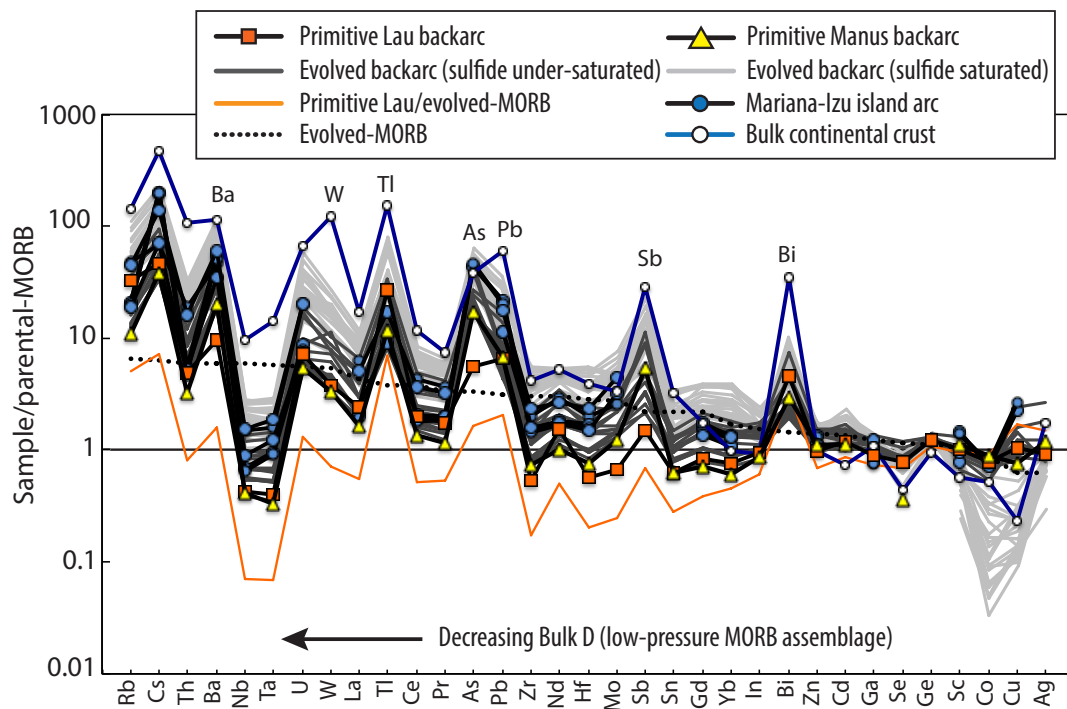


Figure 4: Parental-MORB-normalized trace element patterns. Primitive and evolved BAB basalts^{7, 8, 25}, Mariana-Izu island arc magmas²⁸⁻³¹ and the bulk continental crust²⁶ have comparable trace element patterns. The orange line shows the

551 composition of the primitive Lau BAB normalized to evolved-MORB rather than
552 parental-MORB, demonstrating average-MORB (N-MORB) and evolved-MORB are
553 inappropriate for comparative geochemistry. Element ordering is determined by bulk
554 partitioning (slopes) during MORB differentiation, because partitioning information
555 required to accurately define the ordering in the mantle peridotite assemblage are
556 unavailable. Of the CSE, only W, Tl, As, Pb, Mo, Sb and Bi are mobile during
557 subduction.
558

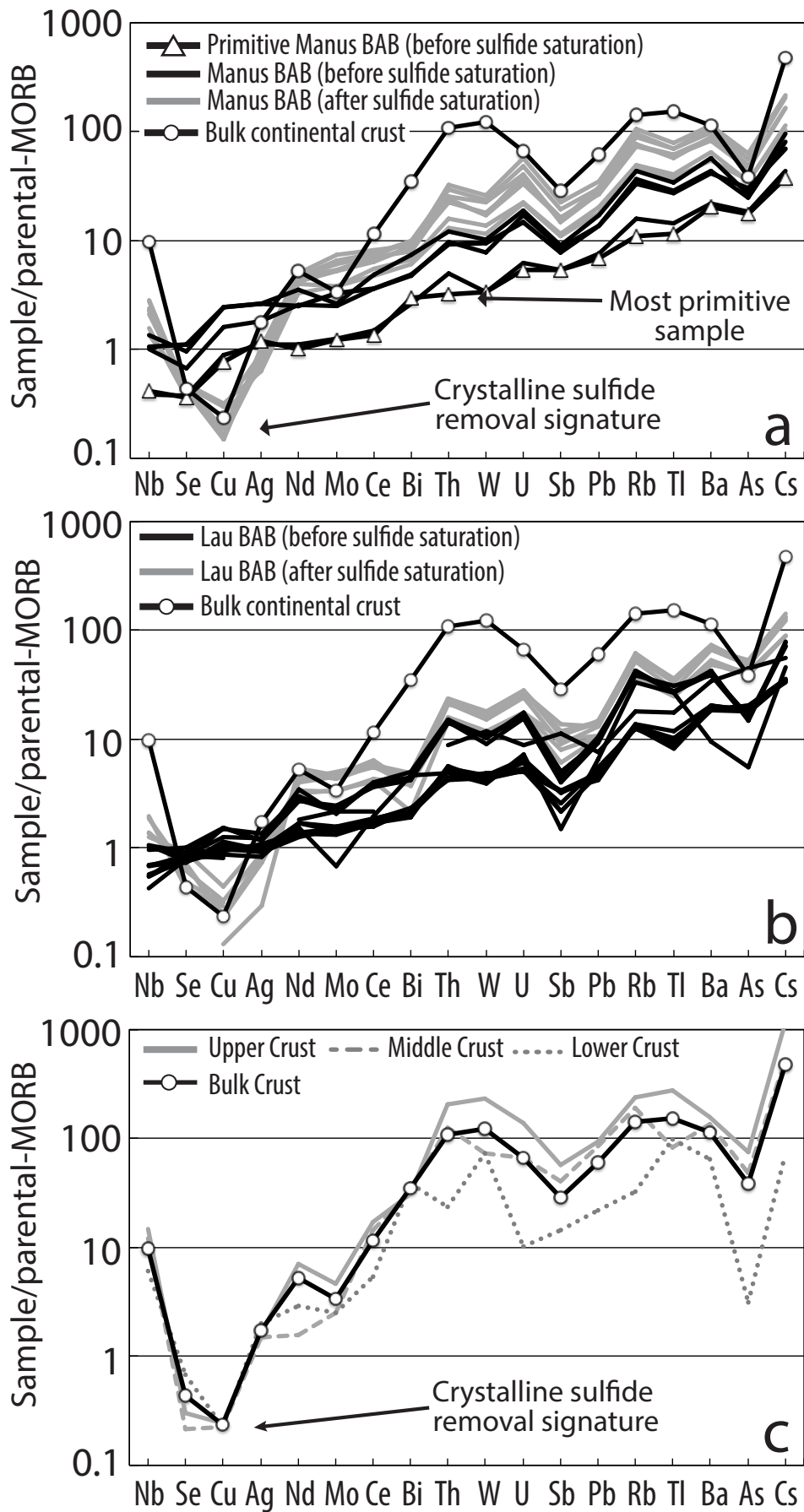


Figure 5: Parental-MORB normalized trace element patterns. The bulk continental crust estimate²⁶ is compared to a-b) sulphide under-saturated (black lines) and sulfide-saturated BAB samples (grey lines) from a) the Manus BAB^{7, 25} b) the Lau BAB⁸. Element ordering is defined by the enrichments in the primitive Manus sample compared to parental-MORB. c) All layers of the continental crust show patterns similar to sulphide-saturated BAB magmas, indicating the majority of convergent margin magmas reach sulphide saturation prior to ascent to higher crustal levels.

METHODS

Data filtering

Source data for Figures 1-5 and Supplementary Figure 1 are provided with the paper. The MORB dataset of Jenner and O'Neill²¹ was used to constrain the relative bulk-D of the CSE during the petrogenesis of MORB, excluding plume-proximal samples (see^{21, 25}) and highly evolved samples with <6 wt.% MgO (see^{33, 34}). As discussed in Jenner and O'Neill²¹ (their Figures 2 and 3) and Jenner et al.²⁵ (their Figure 9), plume-proximal samples have elevated [Cu] at a given [MgO] compared to the majority of the MORB array. Hence, plume-proximal samples appear to either be sulfide under-saturated or fractionate a smaller percentage of sulfide melt during differentiation compared to 'typical' MORB. Consequently, these samples were not considered to be representative of the typical behaviour of the CSE during the petrogenesis of MORB and were filtered from the dataset prior to calculating the slopes and the primitive- and evolved-MORB compositions.

Data fitting

The slopes, b , by which the log-mean content of a given element, $[M]$, changes with $[MgO]$, that is, $d(\log[M])/d[MgO]$, and the predicted abundances of $\log[M]_{10}$ at $[MgO] = 10$ (average primitive-MORB) and $\log[MgO]_{7.6}$ at $[MgO] = 7.6$ (average erupted MORB) were obtained from the least squares best-fit to the Equation:

$$\log[M]_{10} = \log [M]_o + b([MgO]-10) \quad (E1a)$$

$$\log[M]_{7.6} = \log [M]_o + b([MgO]-7.6) \quad (E1b)$$

respectively, where logarithms are to the base 10. The parental MORB and evolved MORB compositions converted back to ‘normal’ numbers are presented in Supplementary Table 1, together with the corresponding slopes.

The standard error of the slope, S_b , is calculated using:

$$s(\log[M])/\sqrt{\sum([MgO] - \overline{[MgO]})^2} \quad (E2)$$

Where $s(\log[M])$ is the standard error of the regression (termed ‘variability’ by O’Neill and Jenner^{33, 34}), given by:

$$s(\log[M]) = \sqrt{(\sum(\log[M] - \log[M]_o - b [MgO])^2)/(n-2))} \quad (E3)$$

There is a systematic increase in $s(b)$ and $s(\log[M])$ with decreasing slope (Supplementary Table 1 and O’Neill and Jenner³³, their Figure 3), because variability

in erupted MORB compositions, inherited during both mantle and crustal processes, increases with incompatibility (see Refs.^{33, 34}, for detailed discussion). The elevated $s(b)$ and $s(\log[M])$ for Re, Pt, Au, As and Sb can be attributed to the low contents of each of these elements (near limits of detection) and/or interferences on each mass during LA-ICP-MS analysis (see^{13, 51, 52}).

The standard error of $\log[M]_{7.6}$ is calculated using:

$$s(\log[M]_{7.6}) = s(\log[M]) \times \sqrt{(1/n + (7.6 - [\overline{\text{MgO}}])^2) / \sum([\text{MgO}] - [\overline{\text{MgO}}])^2)}$$

(E4)

and likewise for $s(\log[M]_{10})$. Each of the equations listed above can be calculated using the Excel LINEST function. Uncertainties in $[M]_{7.6}$ were calculated using:

$$s[M]_{7.6} = \ln(10) \times [M]_{7.6} \times s(\log[M]_{7.6})$$

(E5)

and likewise for $s[M]_{10}$, and are presented in Supplementary Table S1.

References

51. Jenner, F.E. & O'Neill, H.S.C. Major and trace analysis of basaltic glasses by laser-ablation ICP-MS. *Geochemistry geophysics geosystems* **13**, Q03003 (2012).
52. Jenner, F.E., Holden, P., Mavrogenes, J.A., O'Neill, H.S.C. & Allen, C. Determination of Selenium Concentrations in NIST SRM 610, 612, 614 and

634 Geological Glass Reference Materials using the Electron Probe, LA-ICP-MS
635 and SHRIMP II. *Geostandards and Geoanalytical Research* **33**, 309-317.